General response: We sincerely thank the editor and all the reviewers for their valuable feedback, which we have used to improve the quality of our manuscript. The reviewer comments are provided below in **bold font,** and specific concerns have been numbered. Our responses are given in normal font, and changes/additions to the manuscript are given in blue text.

Responses to Referee #2

General comments

The manuscript describes the analysis of the joint probability of storm surge and the significant wave height caused by tropical cyclones. The analysis was applied to a specific case study (Eastern coast of the Leizhou Penisula and Hainan Island of China).

Although the approach can be interesting, the paper presents several shortcomings related both to the methodology and to the presentation of results. The approach adopted for the description of the analysis is not very detailed. In particular, the description of the numerical models does not allow for an adequate understanding of their performance and the reliability of the results. More details about the setup of the numerical models and the validation result should be provided. Moreover, there is a lack of physical explanation of the phenomena simulated and related results.

Overall, the paper, although interesting, cannot be published in its present form.

Response: We greatly appreciate your suggestions and comments in reviewing the manuscript. Please kindly find the detailed responses and revisons to your comments below.

Specific comments

1. **How many tropical cyclones were used in this study? (line 95: 87, line 109: 119, line 119: 102).**

   Response: Thanks for your comments. As the simulation results of the tropical cyclone storm surge and wave in this manuscript were obtained from different institutions, the number of simulations for historical tropical cyclone storm surges and waves was different, with a total of 119 events for storm surges and 102 events for waves. In this study, 86 tropical cyclone storm surges and waves that simultaneously affected the study area from 1949 to 2013 were finally screened for joint probability analysis. To reduce misunderstanding, we have set the number of TC events to 86 in the revised manuscript.

   Line 77-79: Based on the dataset of surge height (SH) and significant wave height (SWH) of tropical cyclones, we screen 86 historical tropical cyclone (TC) events that simultaneously affected the study area from 1949 to 2013 for joint probability characteristics analysis of storm surge and wave.

   Line 91-93: The TC surge heights (SHs) dataset is obtained from the Ocean University of China, mainly through the Advanced Circulation Model simulation results (ADCIRC) simulations, which includes the SHs of 86 TCs affecting the Leizhou Peninsula from 1949 to 2013 (Liu et al., 2018; Li et al., 2016).

   Line 105-106: The TC significant wave heights (SWHs) dataset is obtained from the Ocean University of China, mainly through the SWAN model, and includes the SWHs of 86 TC events affecting the Leizhou Peninsula from 1949 to 2013 (Li et al., 2016).

2. **To understand the result of the numerical models, the authors should provide a depth map of the study area.**

   Response: Thanks for your suggestions. We agree that a depth map is needed. So we add a sentence to show the source of a depth map of the study area (Liu et al., 2018). In this study, we focus more on the joint probability analysis using the simulation results of tropical cyclone storm surges and waves, where the storm surge and wave datasets are derived from the model simulation results of the Ocean University of China, and the corresponding references (Liu et al., 2018; Li et al., 2016) are cited in the manuscript, and the source of the data is indicated and acknowledged in the acknowledgments.

   Line 91-94: The TC surge heights (SHs) dataset is obtained from the Ocean University of China, mainly through the Advanced Circulation Model simulation results (ADCIRC) simulations, which includes the SHs of 86 TCs affecting the Leizhou Peninsula from 1949 to 2013 (Liu et al., 2018; Li et al., 2016). For the study area, a water depth map is provided in the past study (Liu et al., 2018).

   Line 105-106: The TC significant wave heights (SWHs) dataset is obtained from the Ocean University of China, mainly through the SWAN model, and includes the SWHs of 86 TC events affecting the Leizhou Peninsula from 1949 to 2013 (Li et al., 2016).

   Line 413-415: We are grateful to Xing Liu of the Ocean University of China for providing

the simulation data of storm surges and waves for historical tropical cyclone events.

Liu, X., Jiang, W., Yang, B., and Baugh, J.: Numerical study on factors influencing typhoon-induced storm surge distribution in Zhanjiang Harbor, Estuar. Coast. Shelf Sci., 215, 39–51, https://doi.org/10.1016/j.ecss.2018.09.019, 2018.

Li, J., Fang, W., Zhang, X., Cao, S., Yang, X., Liu, X., and Sun, J.: Similar tropical cyclone retrieval method for rapid potential storm surge and wave disaster loss assessment based on multiple hazard indictors, Mar. Sci., 40, 49–60, https://doi.org/10.11759/hykx20151104001, 2016.

3. **The authors do not provide the criteria adopted for the generation of the unstructured grid. Were there any convergence tests?**

   Response: SMS software is used in the model to construct a refined and unstructured grid of offshore of the eastern Leizhou Peninsula. A description of the unstructured grid can be found in the literature (Li et al., 2016), as follows:

   A nesting technique is used in this study to distinguish the local atmospheric forcing from the remote atmospheric forcing. By setting an open boundary for the subdomain, we were able to force the subdomain either with or without remote atmospheric forcing. This can also balance the demands of high resolution in ZH and the associated computation costs. As shown in Fig. 1, the full domain covers most of the South China Sea, and the subdomain only occupies a small area surrounding ZH. There are 36367 elements and 18606 nodes in the full domain with the resolution varying from 0.7 to 20 km. In the subdomain, there are 27487 elements and 14607 nodes with the resolution varying from 0.18 to 3 km. The time step used in the model is 3 s.

4. **How were the boundary conditions of the numerical models set?**

   Response: Thanks for your question. The following is a description of the boundary conditions in the literature (Li et al., 2016).

   The full domain is driven by atmospheric forcing at the surface and surge elevation inversed from the sea surface atmospheric pressure at the open boundary. The boundary condition to force the surge in the subdomain is the time series of the water level on each boundary nodes, which includes both the tide elevation of 8 major constituents (M2, S2, N2, K2, K1, O1, P1, and Q1) in that area from OSU Tidal Prediction Software (Egbert and Erofeeva, 2002) and the surge elevation extracted from the full domain results. A tide model is also run in the subdomain with only the tidal signal including the same 8 constituents being applied at the open boundary.

5. **Which are the governing equations of the two models? Why were these models selected?**

   Response: The wave model has entered a mature stage of development. The third-generation wave model SWAN has the advantage of high computational accuracy and stability and has been widely used in numerical simulations of offshore waters. We added related info in the revised manuscript.

In addition, the ADCIRC model integrates the effects of various boundary conditions and external forcing, uses triangular grids with different resolutions, making it more computationally efficient and well applicable in numerical simulations, and is widely used in areas such as marine, coastal and small-scale estuary systems.

Therefore, the SWAN and ADCIRC model simulations of tropical cyclone waves and storm surges were chosen for the joint probabilistic analysis.

The governing equations of the SWAN model are as follows (https://link.springer.com/article/10.1007/s10915-011-9555-6):

$$\frac{\partial N}{\partial t}+\frac{\partial}{\partial \lambda}[(c_\lambda+U)N]+cos^{-1}\varphi\frac{\partial}{\partial \varphi}\left[\left(c_\varphi+V\right)N\cos\varphi\right]+\frac{\partial}{\partial \theta}[c_\theta N]+\frac{\partial}{\partial \sigma}[c_\sigma N]=\frac{S_{tot}}{\sigma}$$

The wave action density $N(t,\lambda,\varphi,\sigma,\theta)$ is allowed to evolve in time (t), geographic space (λ,φ) and spectral space (with relative frequencies σ and directions θ), (c_λ,c_φ) is the group velocity, (U,V) is the ambient current, and c_θ and c_σ are the propagation velocities in the θ- and σ- spaces, the source terms S_{tot} represent wave growth by wind.

ADCIRC computes water levels via the solution of the Generalized Wave Continuity Equation (GWCE), which is a combined and differentiated form of the continuity and momentum equations:

$$\frac{\partial^2\zeta}{\partial t^2}+\tau_0\frac{\partial\zeta}{\partial t}+Sp\frac{\partial\widetilde{J_\lambda}}{\partial\lambda}+\frac{\partial\widetilde{J_\varphi}}{\partial\varphi}-SpUH\frac{\partial\tau_0}{\partial\lambda}-VH\frac{\partial\tau_0}{\partial\varphi}=0$$

and the currents are obtained from the vertically-integrated momentum equations:

$$\frac{\partial U}{\partial t}+S_pU\frac{\partial U}{\partial\lambda}+V\frac{\partial U}{\partial\varphi}-fV=-gS_p\frac{\partial}{\partial\lambda}\left[\zeta+\frac{P_s}{g\rho_0}-\alpha\eta\right]+\frac{\tau_{s\lambda,winds}+\tau_{s\lambda,winds}-\tau_{b\lambda}}{\rho_0H}+\frac{M_\lambda-D_\lambda}{H}$$

$$\frac{\partial V}{\partial t}+S_pU\frac{\partial V}{\partial\lambda}+V\frac{\partial V}{\partial\varphi}-fU=-g\frac{\partial}{\partial\varphi}\left[\zeta+\frac{P_s}{g\rho_0}-\alpha\eta\right]+\frac{\tau_{s\varphi,winds}+\tau_{s\varphi,winds}-\tau_{b\varphi}}{\rho_0H}+\frac{M_\varphi-D_\varphi}{H}$$

where $H=\zeta+h$ is total water depth; ζ is the deviation of the water surface from the mean; h is bathymetric depth; $Sp=cos\varphi_0/cos\varphi$ is a spherical coordinate conversion factor and φ_0 is a reference latitude; U and V are depth-integrated currents in the $x-$ and $y-$ directions, respectively; $Q_\lambda=UH$ and $Q_\varphi=VH$ are fluxes per unit width; f is the Coriolis parameter; g is gravitational acceleration; Ps is atmospheric pressure at the surface; ρ_0 is the reference density of water; η is the Newtonian equilibrium tidal potential, and α is the effective earth elasticity factor; $\tau_{s,winds}$ and $\tau_{s,waves}$ are surface stresses due to winds and waves, respectively; τ_b is bottom stress; M are lateral stress gradients; D are momentum dispersion terms; and τ_0 is a numerical parameter that optimizes the phase propagation properties.

Line 106-108: The SWAN model has the advantage of high computational accuracy and stability and has been widely used in numerical simulations of offshore waters.

Line 94-95: The ADCIRC model integrates the effects of various boundary conditions and

external forcing and uses triangular grids with different resolutions, making it more computationally efficient and well applicable in numerical simulations.

6. **Provide more details about the validation of the numerical results (station location, comparison of the storm surge and the significant wave height, performance parameters, etc.).**

   Response: Thanks for your suggestions. As the tropical cyclone storm surge and wave datasets used in this study are obtained from the Ocean University of China. Following your suggestion, the physical metrics, spatial and temporal resolution, and model simulation accuracy are briefly described in this manuscript. As for the validation of the numerical results, the locations of the validation sites are added in Figure 1b in this manuscript, and the validation details can be found in the reference (Liu et al., 2018; Li et al., 2016).

   Line 94-101: The simulation results are the total water level after the superposition of the water gain caused by a tropical cyclone and astronomical tide, and the simulation time step is 30 minutes. To improve the simulation accuracy and computing speed of the hot spot area, the model adopts a triangular grid with nested small- and large-area grids and the resolutions of different area grids are set in a gradual resolution range from 0.0039° to 0.3°. Comparing the simulation values with the measured surge height at the observation sites, we discover that the absolute standard error is 47 cm, the relative standard error is 22%, and the simulation results are similar to the observed values in most cases.

   Line 109-114: The model also uses a triangular grid with nested small- and large-area grids and gradual resolution, but the nodes' scopes and locations differ from those of the storm surge model. A comparison of the observed data of buoy stations with the simulated values reveals that the unstructured grid can well reflect the wave variation conditions in the sea. In addition, the mean absolute error and root mean square error of the simulated results of the locally encrypted unstructured triangular grid are the smallest, indicating that the data can effectively reproduce the wave distribution during tropical cyclones.

7. **Figure 4. On the East side of Hainan Island, the surge height increased considerably. Is there some physical explanation for such phenomena?**

   Response: Thanks for your suggestion. In the revised manuscript, we have added the appropriate explanation of the spatial distribution of storm surge heights on the eastern side of Hainan Island.

   Line 235-237: As the return period increases, SH shows varying degrees of growth in each region, and regional differences are more pronounced, with a significant area of development in southeastern Hainan Island, which may be related to the region's location on the edge of the continental shelf and high variability in seafloor topography.

8. **Figure 5: The significant wave height is very high in the offshore region. Is there some physical explanation for such phenomena? It is suggested to consider the effect of the wave breaking.**

   Response: Thanks for your suggestion. The significant wave height in the offshore region

is relatively lower than in distant areas due to wave breaking, which we have explained in the revised manuscript.

Line 240-242: As shown in Figure 5, the SWH near the shore is generally smaller than that in the deep sea and offers a significant decreasing trend as it approaches the coastline. This finding is mainly attributed to the shallow shore depth, island obstruction, wave breaking, and seabed friction attenuation.

9. **It would seem that the effect of the sea level rising due to storm surge was not considered in the numerical simulation conducted with SWAN. If this is true, in the intermedia and shallow water the results are likely to be unreliable.**

Response: Great thanks to the reviewer for pointing out this. It is indeed not considered when modeling the wave. We also realized that the limitation of this wave dataset would introduce uncertainty in the joint probability estimation. In the meantime, it is challenging to simulate the wave again for this study. In order to inform the readers of this fact, we explained the limitation of this dataset in the data section. And in the discussion section, the impact of this limitation is discussed.

Line 114-115: It shall be noted that the effect of sea level rise due to storm surge was not taken into account during SWH simulation, which will influence the accuracy of SWHs, especially in intermedia and shallow water.

Line 398-405: The joint probabilistic analysis of storm surges and waves in the current study has some limitations, and much work needs further improvement and refinement, including the following: (1) In addition to the two most commonly used indicators, SH and SWH, the contribution of other indicators to the hazard assessment of tropical cyclone storm surge and wave should be explored. (2) Sea level rise due to storm surges is taken into account in the numerical modeling of waves, to minimize errors in the simulation of SWHs in intermediate and shallow water. In addition, the uncertainty of the bivariate joint probability distribution is investigated in depth. (3) The random sample generation method can be further explored to simulate SHs and SWHs in different scenarios, providing more sample data for conducting joint TC storm surge and wave hazard assessments.

Minor point

1. **Figure 1. Add the location of stations used for the validation of the models.**

Response: Thanks for your suggestion. We added the location of the verification stations in Figure 1 (b).

Line 87-89:

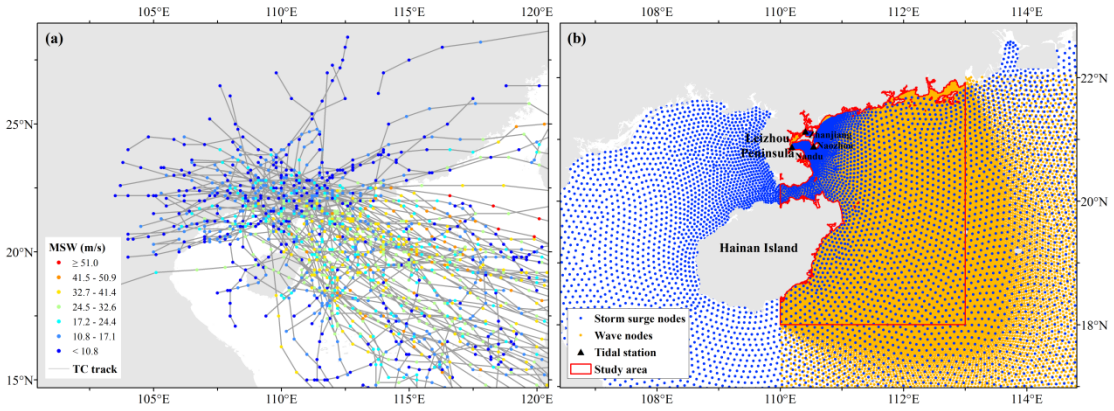

Figure 1: Best track and MSW of 86 TCs in this study from 1949 to 2013 (a) and the study area for the joint probability analysis of storm surges and waves of TCs (b).

2. Triangular network -> triangular grid.

Response: Thanks for the suggestion. We have modified the phrase "triangular network" to "triangular grid" in the revised manuscript.

Line 74-76: Based on the location of the nodes of the triangular grid in the storm surge (Section 2.3) and wave datasets (Section 2.4), we select the region with a dense distribution of both as the study area, and the finalized spatial range is 110°E - 113°E, 18°N - 22°N (Figure 1b).

Line 97-99: To improve the simulation accuracy and computing speed of the hot spot area, the model adopts a triangular grid with nested small- and large-area grids and the resolutions of different area grids are set in a gradual resolution range from 0.0039° to 0.3°.

Line 109-110: The model also uses a triangular grid with nested small- and large-area grids and gradual resolution, but the nodes' scopes and locations differ from those of the storm surge model.

Line 112-114: In addition, the mean absolute error and root mean square error of the simulated results of the locally encrypted unstructured triangular grid are the smallest, indicating that the data can effectively reproduce the wave distribution during tropical cyclones.

Line 203-205: Since the density and location of the triangular grid in the storm surge model and wave model differ, we use the nodes of the storm surge triangular grid as the benchmark and use the wave node closest to each storm surge node as the wave simulation result based on the nearest neighbor method.

3. Table 1. Add the definitions of u and v.

Response: Thank you for the suggestion. We have added the definitions of u and v in the revised manuscript.

Line 154: u and v are uniform (0,1) random variables (Nelsen, 2006).

Nelsen R B. An introduction to copulas[M]. 2nd Edition. New York, USA: Springer, 2006.